

# Physico-mechanical and Biodegradability Study of *Mimusops elengi* Seed Shell Powder Filled PVOH Films Produced through Membrane Casting Method

Wuan Chien Tan,<sup>a</sup> Muniyadi Mathialagan,<sup>a,\*</sup> and Zhong Xian Ooi<sup>b</sup>

The development of biobased-plastic through natural filler addition into polymers has been the best method to resolve numerous environmental problems caused by overconsumption and the increasing waste disposal of non-degradable plastic films. This article produced biodegradable polyvinyl alcohol (PVOH) films by adding *Mimusops elengi* seed shell powder (MESSP) as a filler. The membrane casting method was used to develop the films instead of using the commercially studied solution casting method to avoid inconsistency in the thickness of the casted films. Increasing the MESSP loading enhanced the tensile modulus, resistance towards water absorption, and biodegradability of the PVOH/MESSP films. However, the tensile strength and elongation at break were reduced compared with the unfilled PVOH film. Fourier transform infrared (FTIR) analysis confirmed the reduction of intermolecular bonding between the MESSP and PVOH with increasing the MESSP loading, which is responsible for the reduction in tensile strength, deformability and water absorption of the films. After soil burial exposure, unfilled PVOH films experienced swelling due to water absorption, and there was no evidence of bio-degradation after 9 weeks of exposure. Meanwhile, the PVOH/MESSP films were prone to microorganism activity and biodegradation can be seen as early as 3 weeks after exposure to soil.

*Keywords:* Polyvinyl alcohol; *Mimusops elengi*; Tensile properties; Water absorption; Biodegradability

*Contact information:* a: Department of Petrochemical Engineering, Faculty of Engineering and Green Technology, Universiti Tunku Abdul Rahman, Jalan Universiti, Bandar Barat, 31900 Kampar, Perak, Malaysia; b: Department of Chemical Science, Faculty of Science, Universiti Tunku Abdul Rahman, Jalan Universiti, Bandar Barat, 31900 Kampar, Perak, Malaysia;

\*Corresponding author: mathialagan@utar.edu.my

## INTRODUCTION

Plastics are widely used to substitute for other material such as metal and glass due to their light weight, low cost, and desirable properties. The ductility of plastics makes them unique, and they can be made in many forms and shapes for a wide range of applications. Plastic films made of polymers of petroleum feedstock are flexible in nature and used commonly as grocery bags and general-use packaging materials. Other types of rigid plastics are used as food and beverage containers. Packaging applications govern approximately 39.6% of the plastics industry, which is the largest sector in total plastics demand due to the superior barrier properties of plastic against moisture and air (Marsh and Bugusu 2007). However, high demand and over consumption of non-degradable, petroleum-based plastics causes high pollution rates upon disposal. The generation of plastic waste is far greater than the amount of plastic being recovered or recycled. The collection, identification, sorting, and processing of different kinds of plastics during

recycling are time consuming and generally not economical. Due to the non-degradable nature, petroleum-based plastic films are generally disposed directly into the land and burned openly as a more convenient and low cost method. Both of these methods contribute to the emission of greenhouse and other hazardous gases into environment as well as land scarcity in many small countries (Tardif 2013).

Natural filler is a degradable component and is usually introduced into plastic materials as reinforcement material or to impart biodegradability into the plastics (Chauhan and Chauhan 2013). Biocomposites or biobased-plastics are developed by incorporating natural fillers or fibers into non-degradable polymers. Biobased-plastics can decrease the net amounts of carbon dioxide emissions during manufacturing, and they undergo biodegradation due to microorganism activity in organic matter without leaving any toxic residue in the environment (Nakasaki *et al.* 2000). Hence, biobased-plastics can be used as an alternative to petroleum-based plastic films for packaging applications. This could help to reduce the consumption of non-degradable polymers as packaging materials and minimize the environmental problems caused by the landfilling of plastic films (Tardif 2013). Numerous studies on the development of biocomposites and biobased-plastics using natural fillers such as starch, fruit waste, pineapple leaf, and kenaf have been conducted (Ramaraj 2006; Orchi 2008; Ooi 2011b; Kalambettu *et al.* 2014). Ooi *et al.* (2017) reported on the preparation and properties of oil palm ash filled polyvinyl alcohol (PVOH) films through the solution casting method. The addition of oil palm into PVOH enhanced the resistance towards water absorption and the biodegradability of the films. However, the tensile properties of the films were reduced with the addition of oil palm ash. Moreover, the thickness of the films produced through the commercially studied solution casting method was not consistent and may affect the overall properties of the films produced (Ooi *et al.* 2017). Thus, the membrane casting method was used to develop the films, which uses a thickness controller to spread the PVOH solution into a more consistent thickness.

A new natural filler known as *Mimusops elengi* seed shell powder (MESSP) was introduced in this project to prepare the biodegradable plastic films. *Mimusops elengi* is a ubiquitous evergreen tree that grows in India. It belongs to the Sapotaceae family and is commonly named Spanish cherry or Bullet wood in English. The height of the Bakul tree is around 20 to 30 m. The hard and tough properties of the central wood make it an excellent timber. The heartwood is valuable and used as the construction material for temples in India to build ornate pillars, ceilings, windows, and doors. The flowers of the Bakul tree are star-shape and yellowish-white in color with a pleasant smell. The ovoid shape of the berry is 2.5 cm long. The ripe berries are sweet and edible. Being a neglected fruit, the information regarding the composition of the fruit is scarce.

*Mimusops elengi* is widely used in India for daily applications. The fruit is edible, whereas the oil extracted from the seed is used for cooking. The dried flowers are used as a filling in pillows due to the fragrance of the flower, which can last a long time. The flowers are also used to make necklaces for decoration (Fern 2017). *Mimusops elengi* is well known in India due to its high value in traditional medicinal practices. There has been extensive research regarding the application of *Mimusops elengi* in biological and medical practices. Tannin, saponin, quercitol, d-mannitol, quercetin, alkaloids, and taraxerol are the active components embedded in different parts of *Mimusops elengi* (Baliga *et al.* 2011). According to Kadam *et al.* (2012), the bark, fruit, leaves, seed, and flowers extracted from the plant have pharmacological or toxicological effects. Muniyadi *et al.* (2018) introduced MESSP as a new bio-filler in producing polypropylene (PP) biocomposites; the addition of MESSP has increased the tensile properties up to 10 wt% MESSP compared with

unfilled PP. However, the hydrophilic nature of MESSP results in low adhesion between the PP and the MESSP.

In this research, MESSP was introduced as a filler in PVOH to develop a new biobased-plastic. Good compatibility between MESSP and PVOH was achieved due to the hydrophilic nature of both PVOH and MESSP. The membrane casting method was used to develop the plastic film instead of the commonly used solution casting film to reduce the inconsistency in the thickness of the films produced. The tensile properties, water, and biodegradability through a soil burial test over 3, 6, and 9 weeks were examined.

## EXPERIMENTAL

### Materials

The PVOH polymer matrix was supplied by Alfa Aesar Chemical manufacturing company (Ward Hill, MA, USA). The chemical abstract service (CAS) registry number is 9002-89-5. The PVOH resin in powder form used was 98 to 99% hydrolysed. It has the average molecular mass in the range of 89,000 to 98,000 g mol<sup>-1</sup> and a density of 1.269 g/cm. The PVOH product is a white or cream colored granular powder. It is a water-soluble synthesized polymer with -OH bonds at the backbone. The chemical and physical properties are strongly dependent on the percentage of hydrolysis and the molecular weight. The extent of the hydrolysis and polymerization affect the solubility of PVOH in water. Its glass transition and melting temperature are, respectively, 85 °C and 240 °C (Campos *et al.* 2011).

*Mimusops elengi* seed shell powder (MESSP) was the filler added to the matrix. It was produced from the seeds of ripe fruits of *Mimusops elengi* plants from Taman Kampar Perdana, Kampar, Perak (Google map coordinate: 4°20'20"N, 101°9'9"E). The seeds were gently squeezed from ripe *Mimusops elengi* fruit and exposed to sunlight for 4 to 5 h daily for one week until they changed to a brownish color, indicating that they were dried. Dried seed shells were obtained after removing the kernel. The dried seed shells were cleaned by immersion in distilled water with a magnetic stirrer at 300 rpm 80 °C for 2 h. The ratio of distilled water to seed shell was at least 1:3 by volume. The cleaned seed shells were tossed using a sieve and oven-dried (Memmert, Schwabach, Germany) at 80 °C for 24 h. The seed shell was grinded and sieved to < 45 µm particle size using a sieve shaker (RX-29-10) to obtain MESSP (Muniyadi *et al.* 2018).

### PVOH/MESSP film preparation

PVOH/MESSP films were prepared through solution mixing of MESSP in PVOH. First, 20 g of PVOH was weighed and dissolved in 180 mL of deionized water in a 250 mL conical flask.

**Table 1.** Compounding Formulation of PVOH/MESSP Films

Film Codes	Composition		MESSP Loading (wt %)
	PVOH (g)	MESSP (g)	
PVOH/MESSP 100/0	20.0	0.0	0
PVOH/MESSP 95/5	19.0	1.0	5
PVOH/MESSP 90/10	18.0	2.0	10
PVOH/MESSP 85/15	17.0	3.0	15
PVOH/MESSP 80/20	16.0	4.0	20

The solution was heated at 110 °C with a constant stirring speed until the PVOH was fully dissolved, which was approximately 2 h and 30 min. For the MESSP filled PVOH solution, the MESSP was added slowly into the conical flask after 30 min of dissolving the PVOH in the deionized water. The solutions were continuously heated and stirred for 2 h (Ooi *et al.* 2017). The compounding formulation of the PVOH/MESSP films is shown in Table 1. The prepared solutions were cast into thin films using the membrane casting machine and left to dry overnight.

## Methods

### *Characterization of MESSP and PVOH/MESSP films*

A Fourier transform infrared analysis (with attenuated total reflection) with a spectrophotometer (ATR-FTIR; Perkin Elmer RXI IR, Waltham, MA, USA) was used to identify the types of chemical bonds and functional groups in the MESSP, PVOH, and PVOH/MESSP films. The chemical functionality was analyzed to clarify the bonding or interaction between the PVOH and MESSP. The absorbance bands were observed at wavelengths from 4000 cm<sup>-1</sup> to 400 cm<sup>-1</sup> with 16 times scanning at a resolution of 4 cm<sup>-1</sup>.

The morphology of the MESSP and casted PVOH/MESSP films were studied using scanning electron microscopy (SEM; JEOL JSM 6701-F, Akishima, Japan). Prior to scanning, the samples were placed on a disc and held in place using double-sided carbon tape, and then they were sputter coated with a thin layer of platinum. The approximate thickness of the layer of the coating was 15 nm with the density of 21.45 g/cm<sup>3</sup> using a sputtering machine (JFC-1600, JEOL) to avoid electrostatic effects, which may cause poor resolution in the scanning process. The SEM analysis was carried out at an accelerating voltage of 4 kV with a working distance of 10 mm depending on the focal point. The analyses determined the shape and surface morphology of MESSP and PVOH as well as the quality of the MESSP coated on the PVOH film. After tensile testing, the fracture surfaces of the film were also analyzed to study the MESSP dispersion on PVOH, interfacial adhesion between MESSP, and PVOH as well as the fracture mode. The surface morphology of PVOH and MESSP/PVOH films were investigated again after the soil burial test to analyze the biodegradability properties.

### *Water absorption measurement*

PVOH/MESSP films were cut into dumbbell shaped specimens using a dumbbell cutter (Leader Technology Scientific (M) Sdn. Bhd., Balakong, Malaysia). A water absorption test was carried out according to ASTM D 570-98 (2010). The samples were oven-dried for 24 h at 80 °C. Next, the weights of the samples ( $W_i$ ) were determined using an electronic analytical and precision balance (Sartorius M-pact AX224, Sartorius AG, Germany). The films were immersed in the distilled water at room temperature, 25 °C, and kept in a dark place for 72 h. After 72 h, the surface of the samples were wiped with a tissue and weighed again. The weight of the samples after the swelling test ( $W_f$ ) was recorded. The water absorption resistance ( $W_a$ ) of PVOH/MESSP film was calculated as the change in weight of the film in distilled water. A lower  $W_a$  value indicates that the PVOH/MESSP film has higher water resistance; it was calculated as shown in Eq. 1 (Ghani and Ahmad 2011).

$$W_a = \frac{W_i - W_f}{W_i} \times 100\% \quad (1)$$

### Tensile test

The tensile properties of PVOH/MESSP films such as elastic modulus, ultimate tensile strength, and elongation at break were examined according to the ASTM D638-14 (2014) standard under ambient conditions. The tensile test was conducted by using a light-weight tensile tester (Tinius Olsen H10KS-0748, Salfords, UK) with a load cell of 450 N at a crosshead speed of 20 mm/min until the specimen fractured. The specimen was subjected to 1200 mm of extension range with a 26 mm of gauge length. Prior to the tensile test, the films were cut into dumbbell shaped specimens with a dumbbell cutter. Five dumbbell shaped specimens were cut and labeled for each of the different MESSP loading films. The average values of the results for the five repeated specimens were determined for each composition (Ooi *et al.* 2011b).

### Natural soil burial

The soil burial test was conducted according to procedures described by Obasi *et al.* (2013) and Ooi *et al.* (2017). Composted soil was purchased from Success Superior Soil from Jaya Pot Enterprise (Kuala Langat, Malaysia). Plastic film specimens containing different PVA and MESSP compositions were prepared by cutting using a dumbbell cutter and buried in the soil at a depth of 9 cm. The bottom of the plastic container was perforated with a small hole to avoid water accumulation. Same amount of water was added to the soil to maintain the moisture content for all the specimens and placed in an exposed area at the Faculty of Engineering and Green Technology (FEGT), Universiti Tunku Abdul Rahman, Kampar, Perak, Malaysia. To measure the degradation of the plastic films, the initial appearance and weight ( $B_i$ ) of the samples was recorded before being placed into the soil. The samples were removed from soil after 3, 6, and 9 weeks and the surface was wiped with tissue before weighing the final weight. The final appearance and weight after soil burial ( $B_f$ ) were recorded. The weight loss ( $B_L$ ) percentage of the samples was calculated using Eq. 2 (Obasi *et al.* 2013; Ooi *et al.* 2017). The weight loss of the samples was used to determine the degradation rate of the specimens. Furthermore, the morphology of the sample films before and after the soil burial test was examined using SEM.

$$B_L = \frac{B_i - B_f}{B_i} \times 100\% \quad (2)$$

## RESULTS AND DISCUSSION

### Characterization of PVOH/MESSP Films

Figure 1 shows the spectra of unfilled PVOH and MESSP. PVOH has the strong and wide absorbance band at  $3271.71 \text{ cm}^{-1}$ , which confirmed that there are excess of hydroxyl group to form secondary hydrogen bonding with hydroxyl groups from MESSP (Ooi *et al.* 2011a). Spectrum (a) in Fig. 1 shows the asymmetric methyl group; C-H stretching bands appeared at the peaks  $2940.8 \text{ cm}^{-1}$ . Stretching peak appeared at  $1415.2 \text{ cm}^{-1}$  and  $1324 \text{ cm}^{-1}$  were corresponds to C-H bending. There were asymmetrical flexible vibrations peaks of C-O-C, which occurred at  $1142.2 \text{ cm}^{-1}$  and  $1087.4 \text{ cm}^{-1}$ . The main absorbance bands that were corresponding to the PVOH component are tabulated in Table 2. The incomplete removal of acetate groups during the manufacturing of PVOH by the hydrolysis of poly (vinyl acetate) could be the reason for the presence of carbonyl band at  $1656.8 \text{ cm}^{-1}$  (Ooi *et al.* 2011b). The significant peak value observed was the hydroxyl functional group, which confirmed the hydrophilic nature of PVOH.

**Table 2.** FTIR Spectroscopy of PVOH (Stuart 2004)

Spectroscopic Assignments	Wavenumber (cm <sup>-1</sup> )
O-H Stretching	3650 – 3200
C–H Stretching Bands	3000 – 2800
Asymmetric C-H Stretching	2940.8
Methylene Scissoring	1415.9
Methylene Wagging	1328.4
C-O-C Stretching	1142.2 and 1087.4

The ATR-FTIR spectrum as illustrated in Fig. 1 spectrum (b) are similar and consistent with those plant fibers such as kenaf (Bakar *et al.* 2015), hemp fibers (Troedec *et al.* 2008), wheat straw, soy hulls (Alemdar and Sain 2008), and starch (Stuart 2004). The main absorbance bands present in the MESSP were 3340.8 cm<sup>-1</sup>, 1729.5 cm<sup>-1</sup>, 1632.0 cm<sup>-1</sup>, 1239.6 cm<sup>-1</sup>, and 1035.8 cm<sup>-1</sup>. There was a strong and broad stretching band that appeared at 3340.8 cm<sup>-1</sup>, which in the range of 3200 to 3650 cm<sup>-1</sup> corresponded to the stretching -OH group. This could also confirm the polarity of the MESSP where the assumption of the good compatibility between the MESSP fibers and the PVOH matrix could be made. In addition, there was a peak that appeared at 2927.9 cm<sup>-1</sup> within the range of 3000 cm<sup>-1</sup> to 2800 cm<sup>-1</sup>, which was attributed to a weak stretching C-H group. Apart from that, infrared analysis stated that the plants comprised up to 80% of their dry weight of carbohydrate, which included the main components such as cellulose, pectin, and hemicelluloses, all of which could be found in MESSP (Stuart 2004). Table 3 reports on the major mid-infrared bands of common plant carbohydrates.

**Table 3.** Major Mid-infrared Bands of Common Plant Carbohydrates (Stuart 2004)

Carbohydrate Type	Wavenumber (cm <sup>-1</sup> )
Cellulose	1170–1150, 1035
Lignin	1590, 1510
Hemicellulose	1732, 1240
Pectin	1680–1600

The absorbance band around 1730 cm<sup>-1</sup> to 1740 cm<sup>-1</sup> may be attributed to the presence of C=O stretching in the acetyl groups of hemicellulose, and the absorbance peak was found at 1729.5 cm<sup>-1</sup> in MESSP (Alemdar and Sain 2008). Also, the peak located at 1632.0 cm<sup>-1</sup> corresponded to the absorbed moisture by the cellulose (Fan *et al.* 2014). The peak near 1510 cm<sup>-1</sup> that appeared on the MESSP spectrum could be connected with C=C stretching vibration of the aromatic skeletal found in lignin (Shi *et al.* 2012). In addition, the presence of CH<sub>2</sub> symmetric bending of cellulose that existed at the peak 1439 cm<sup>-1</sup> could be found in the infrared analysis. The peak at 1238.9 cm<sup>-1</sup> was attributed to the O-H phenolic group in lignin (Muniyadi *et al.* 2018). The presence of the peak at 1163.6 cm<sup>-1</sup> was corresponded to C-O-C asymmetric stretching in cellulose I and cellulose II whereas the peak at 1035.8 cm<sup>-1</sup> was attributed to the C-O of the alcohol (primary and secondary) stretching vibration of cellulose, lignin, and hemicellulose (Shi *et al.* 2012). On the other hand, in the research of Jeyasundari *et al.* (2016), the ATR-FTIR spectroscopy of *Mimusops elengi* flower extract had a prominent peak at 1050.1 cm<sup>-1</sup>, 1679.9 cm<sup>-1</sup>, and 3501.0 cm<sup>-1</sup> due to C–N stretching (aliphatic amines), C=O stretching, and O–H stretching, respectively, which were similar to the peaks that appeared from the spectrum of MESSP.

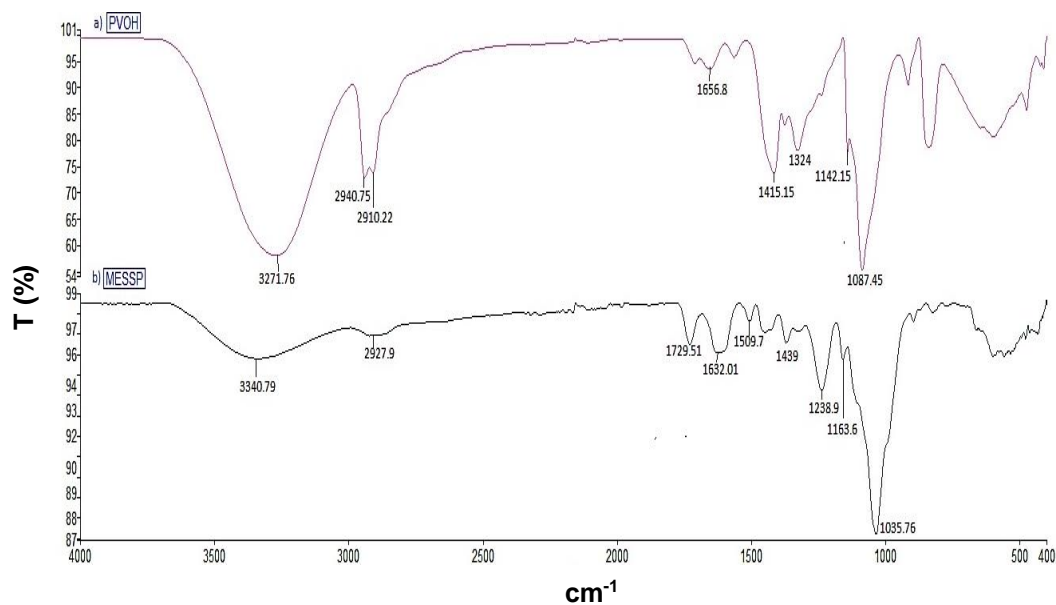


**Fig. 1.** ATR- FTIR spectra of unfilled PVOH and MESSP

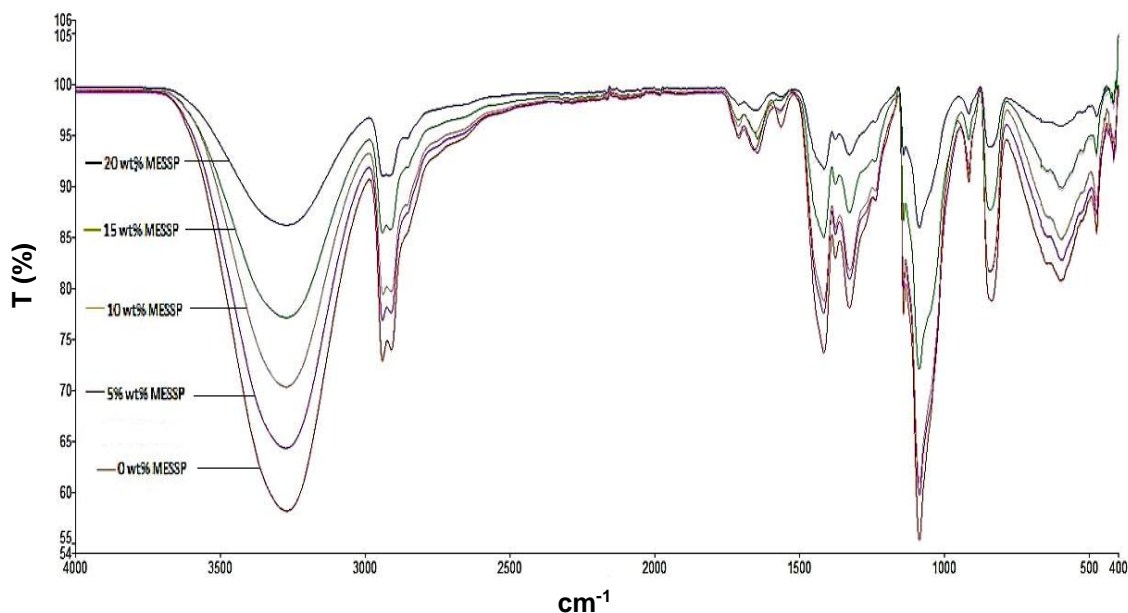


**Fig. 2.** Comparison of overlapping ATR-FTIR spectra on different PVOH/MESSP loading

Figure 2 illustrates the spectra of the PVOH/MESSP films containing different MESSP loading. The vibration peak of the hydroxyl group of unfilled PVOH and MESSP appeared at  $3271.7\text{ cm}^{-1}$  and  $3340.8\text{ cm}^{-1}$ , respectively. However, the PVOH/MESSP films show the peak ranging from  $3272.0$  to  $3272.6\text{ cm}^{-1}$ , which was similar to the hydroxyl band of PVOH. This was due to the higher intensity of the O-H group absorbance in the PVOH as compared to MESSP. Besides that, it can be seen that there were no new peaks that appeared or disappeared when comparing the spectra of unfilled PVOH and PVOH/MESSP films. The result shows that there was no chemical interaction formed between PVOH and MESSP. The shape and location of the characteristic peaks of

PVOH/MESSP films were similar to those of the unfilled PVOH, which indicated that the interactions among the PVOH molecules were dominant as PVOH-PVOH interaction was stronger than those for PVOH-MESSP molecules and MESSP-MESSP molecules. The reduction in intensity of the OH peaks at 3272.0 to 3272.6  $\text{cm}^{-1}$  indicates that the intermolecular hydrogen bonding between the hydroxyl groups in the PVOH/MESSP was getting weaker as the MESSP loading was increased in the films (Ooi *et al.* 2011b).

Figure 3 shows the SEM images of the MESSP particles at 1000 $\times$  magnification. Based on Fig. 3, the MESSP particle is irregular in shape with a flat and smooth surface, and there were no pores or cracks that appeared on the surface. It was expected that there would be good interfacial adhesion between MESSP and PVOH as the smooth and flat surface indicated a large surface area for any possible physical interaction by the interlocking of PVOH chains on the MESSP surface.

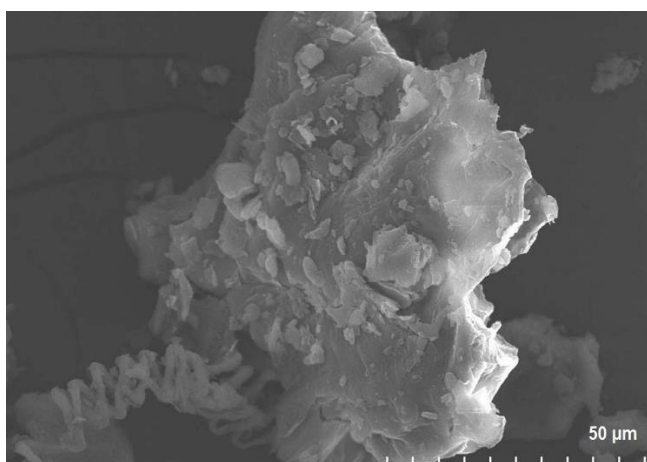


**Fig. 3.** SEM images for MESSP at 1000 $\times$  magnification

### Water Absorption

The water absorption test was conducted on different compositions of PVOH/MESSP films to investigate the water affinity of each blended films. The PVOH is water-soluble and hydrophilic in nature (Kadajji and Betageri 2011). Moreover, the MESSP also showed hydrophilic properties as they possessed the  $-\text{OH}$  hydroxyl group in the structure, as discussed in the results analyzed from ATR-FTIR. Thus, the presence of the hydroxyl group in both the PVOH and MESSP will contribute to the moisture absorption on the blended PVOH/MESSP films. Based on Fig. 4, the water absorption percentage decreased gradually with the addition of the loading of MESSP from 0% to 20 wt%. By comparison, unfilled PVOH films experienced the highest water absorption as compared to the other PVOH/MESSP blends of films. For instance, the reduction of the water absorption percentage of 80/20, PVOH/MESSP blended films was 42% as compared to unfilled PVOH films.

Compared with unfilled PVOH, all other blended films showed decreased water absorption. The unfilled PVOH swelled more in the water and had the highest water absorption rate, which may be due to its having the highest intensity of the hydroxyl group analyzed from the comparison of overlapping ATR-FTIR spectra on different PVOH/MESSP loading. The higher intensity suggested that the unfilled PVOH was more polar and had higher water affinity as the water molecules were attached to  $-\text{OH}$  groups in PVOH polymer chains by hydrogen bonds, which lead to swelling (Baschek *et al.* 1999;

Thakur and Singha 2010; Das and Biswas 2016). The reduction of water uptake by the PVOH/MESSP blended films was associated with the increasing of MESSP loading from 5 to 20 wt%. As reported by Yee *et al.* (2011), natural fibers have less capability to absorb water as compared to PVOH. As the MESSP content was increased in the PVOH/MESSP composite, it corresponded to the decrease of the PVOH content. The MESSP showed lower intensity of the hydroxyl group as compared to unfilled PVOH, which would cause the reduction of the hydrophilic nature to PVOH/MESSP composites. Similar observation was reported in the study by Ooi *et al.* (2017) on the reduction of water absorption by PVOH films with increasing oil palm ash content.

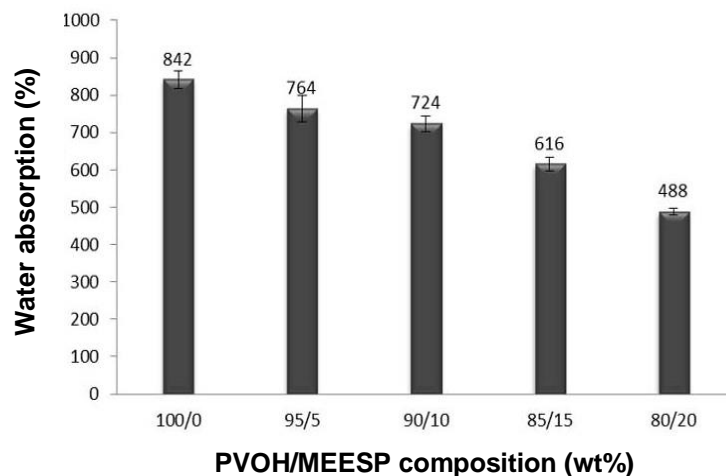


Fig. 4. Water absorption percentage of PVOH/MESSP films

### Tensile Properties

The mechanical tests on tensile strength, elastic modulus, and elongation at break of PVOH/MESSP films were conducted with different MESSP loading. Determination of film stretching is important for packaging applications (Raj and Siddaramaiah 2004). Particle size, shape, and particle distribution affect the mechanical properties of the composite. Additionally, filler loading, filler dispersion, and the interfacial adhesion between the matrix and the filler affect the performance of blended films (Thomas *et al.* 2012; Tan *et al.* 2015).

Figure 5 illustrates the tensile strength and the elongation at break for the different loading of MESSP incorporated in PVOH, where both parameters exhibited the same trends. Obviously, the tensile strength and the elongation at break were decreasing as the MESSP loading increased. The tensile strength was the highest for unfilled PVOH, followed by the increasing of the MESSP loadings from 5% to 20 wt %. This was due to the decreasing of the PVOH matrix content as the PVOH exhibited the ductility properties (Ramaraj 2006). In addition, weak tensile strength and the elongation at break might be due to the weak intermolecular hydrogen bonding between the MESSP filler and PVOH matrix. The supportive evidence was discussed in ATR-FTIR analysis earlier and showed that the intensity of the  $-OH$  groups in the films was decreasing where this proved that bonding between the PVOH and MESSP was weaker for higher loading of MESSP. Similar results were obtained by Suki *et al.* (2013) where PVOH/banana front flour blended films have lower tensile strength with higher banana front flour loading.

Despite the lower tensile strength and elongation at break of the PVOH/MESSP

films compared with unfilled PVOH, the tensile properties of this type of film was within the range for packaging application. For example, the established brand of PLA plastic film such as Biobag L, EcoFilm, EcoWorks 45, Indaco, and Heritage have the tensile strength and elongation at break ranging from 12.2 MPa to 37.3 MPa and 17.7% to 1590%, respectively. Thus, the performance of PVOH/MESSP on tensile strength and elongation at break ranging from 26.8 MPa to 46.2 MPa and 41.9% to 91.1% were still applicable for the film packaging application (Vanstrom 2012).

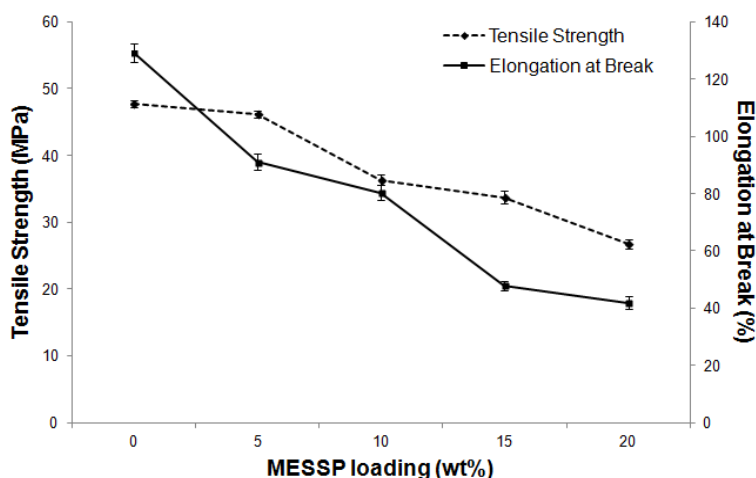


Fig. 5. Tensile strength and elongation at break of PVOH/MESSP blended films

Tensile modulus is the measure of stiffness; in other words, it is the degree of ductility of the filler reinforced polymer (Siracusa *et al.* 2017). Figure 6 shows that the PVOH/MESSP blended films exhibited higher tensile modulus with the increase of MESSP loading. The incorporation of fillers in the films will hinder the mobility of the chains when subjected to force, which in turn increased the brittleness of the blended films. The films with the higher filler content will become stiffer as a result of higher elastic modulus (Gao *et al.* 2014).

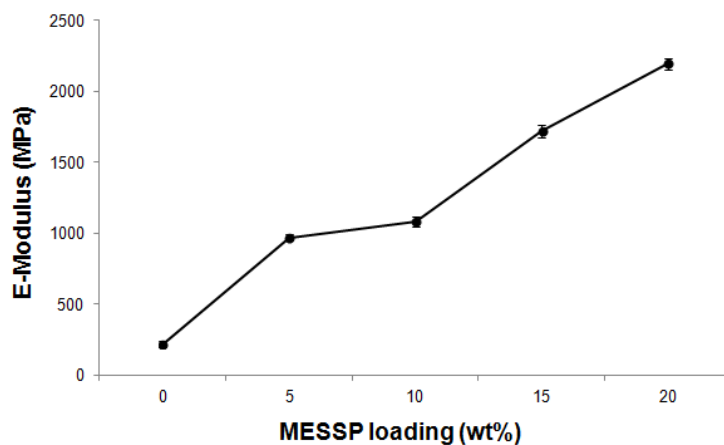
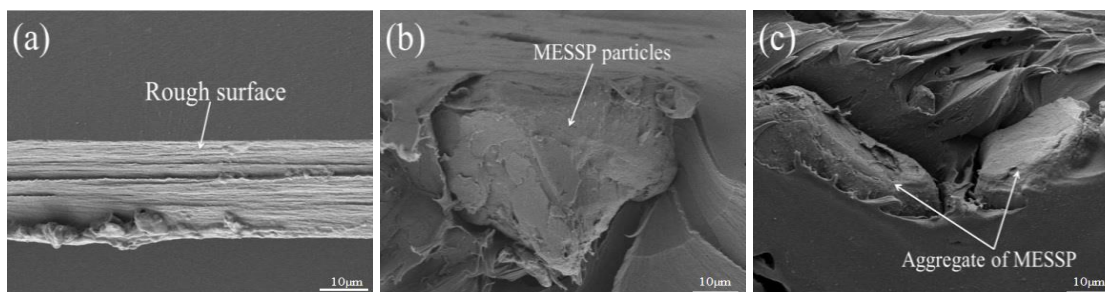


Fig. 6. Elastic modulus of PVOH/MESSP blended films

## SEM Morphology of Tensile Fractured PVOH/MESSP Films

Surface morphology on tensile fracture shows the dispersion and the filler-matrix interfacial interaction of the blended films, which can be used to explain the tensile properties of the composite films. Figure 7 shows the SEM images with a low magnification power of 1500 $\times$  of unfilled PVOH, 10% and 20 wt% of MESSP loading in PVOH matrix. Figure 7a illustrates that the unfilled PVOH have the roughest surface as compared to other blended films. The rough surface was more ductile, which contributed to the good matrix tearing as the mobility of the chains was the highest. Thus, the high deformability allowed more elongation as the elongation at break, as observed for the unfilled PVOH. The elongation could reach up to 129% before breakage. Moreover, adhesion of large particles' size of filler to the PVOH was observed in Fig. 7b. This shows there was lower surface area available for adhesion, which lead to the poor adhesion of MESSP to the PVOH. Hence, to have better filler –matrix interaction, smaller particles' size of the fillers was preferred (Thomas *et al.* 2012). Filler aggregation was shown in Fig. 7c with 20 wt% MESSP loading films. Aggregation of the filler will cause the poor dispersion and non-uniform distribution of MESSP in the PVOH matrix (Kalambettu *et al.* 2014). The MESSP particles that were coarsely dispersed as a consequence of poor filler-matrix interaction. This will reduce the performance of the blended film on the tensile strength and elongation at break parameters (Muniyadi *et al.* 2018). In addition, the aggregation of the MESSP caused the blended films to become more brittle as the tensile modulus was higher for the higher loading of MESSP blended films. The crazing effect would be incurred by the aggregation phenomena where the adhesion of the MESSP with the PVOH matrix phase was destroyed (Ramaraj 2006).



**Fig. 7.** Comparison of surface fracture of PVOH/MESSP at low magnification (1500 $\times$ ). (a) Unfilled PVOH; (b) PVOH/MESSP 90/10 wt %; and (c) PVOH/MESSP 80/20 wt %

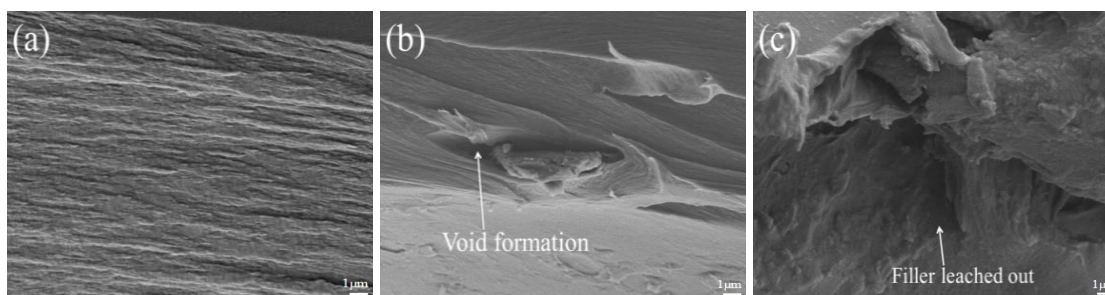


**Fig. 8.** Comparison of surface fracture of PVOH/MESSP at high magnification (5000 $\times$ ). (a) Unfilled PVOH; (b) PVOH/MESSP 90/10 wt%; and (c) PVOH/MESSP 80/20 wt%

Clearer SEM images were obtained by using the higher magnification of 5000 $\times$ , as shown in Fig. 8. The formation of aggregations will form the flaws in the film (Espert *et al.* 2004). When the flaws become bigger in size, the flaws propagate into voids and lead to the poor interfacial interaction as shown in Fig. 8b (Abdul Khalil *et al.* 2009). In addition, the SEM micrograph also shows the filler leached out or pull-out predicted from the low adhesion between the MESSP and PVOH when force was applied, as can be seen from Fig. 8c (Asim *et al.* 2015).

### Soil Burial Degradation

In this research study, the compost soil provided the realistic environment where biodegradation could occur with the presence of microorganisms, outdoor humidity, pH, and temperature in a less controlled manner. The results for the evaluation of the biodegradation of the samples were consecutively collected every three weeks. Percentage of the weight loss and the physical appearance were used to evaluate the extent of the biodegradability of the unfilled PVOH and PVOH/MESSP films.

From the study, unfilled PVOH showed the highest resistance toward the degradation. However, there were 15.0%, 14.8%, and 13.7% weight losses from week 3 to week 9 due to its susceptibility for degradation in water where the films will degrade from water or moisture content in the soil (Kalambettu *et al.* 2014). However, the weight loss trend of PVOH declined, which could be explained by the hydrophilic nature of its features that cause the swelling process of PVOH (Krzeminski and Molisak-tolwinska 1991). Figure 9 shows that there was a slight rise in the weight loss from 13.8% to 16.1% in week 3 as the MESSP's loading was increased from 5% to 20 wt%.

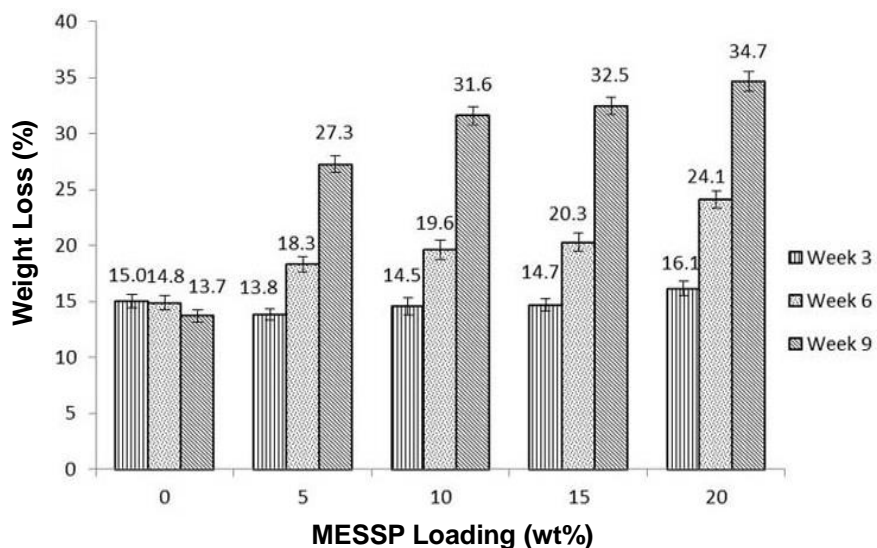
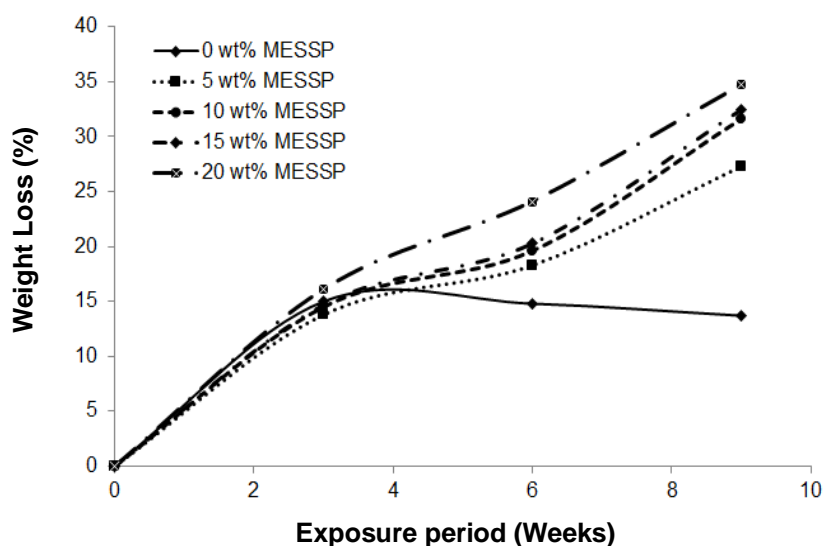


**Fig. 9.** Percentage weight loss of PVOH/MESSP film with respect to increasing of MESSP loading

The observed pattern in week 6 and week 9 may also demonstrate that the PVOH/MESSP blends with higher MESSP loading were associated with the higher degradation rate as the percentage of the weight loss was higher. The PVOH/MESSP 80/20 films showed the highest degradation rate. This can be explained by the presence of MESSP as the natural fiber in the PVOH matrix containing the nutrients for the growth of the microorganism such as potassium, sodium, magnesium, calcium, and iron (Mendez-

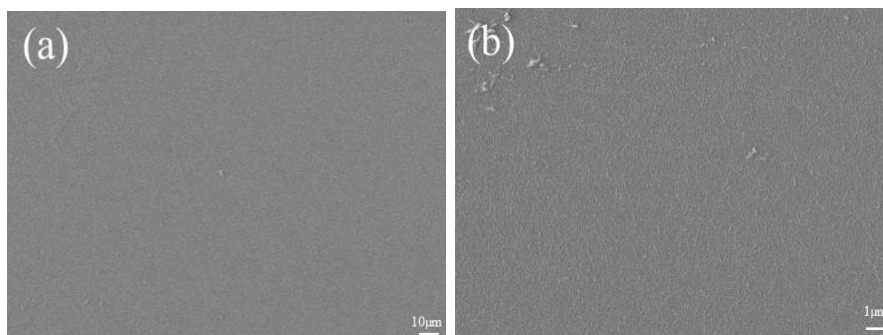
Sanchez *et al.* 2004). An alternative inference could be that the fibers served as capillaries that may have enabled the migration of moisture and microorganism as degradation by microbial attack is the main mode of degradation for natural composites in soil (Kalambettu *et al.* 2014). The incorporation of MESSP in the composites supplied the nutrients and facilitated the microorganism growth by breaking down the fibers.

The results illustrated in Fig. 10 show that as the exposure to soil was prolonged, the weight loss of the composites increased. For instance, the degradation rate was the highest in week 9 for the different loading of the MESSP as compared to week 3 and week 6. This was due to the higher microbial development and the microbial degradation over cellulose and hemicellulose and increased the damages to the films. In short, the longer the prolonged time and the higher loading of MESSP films exhibited a higher degradation rate as evident by the associated increase in the molecular weights loss.



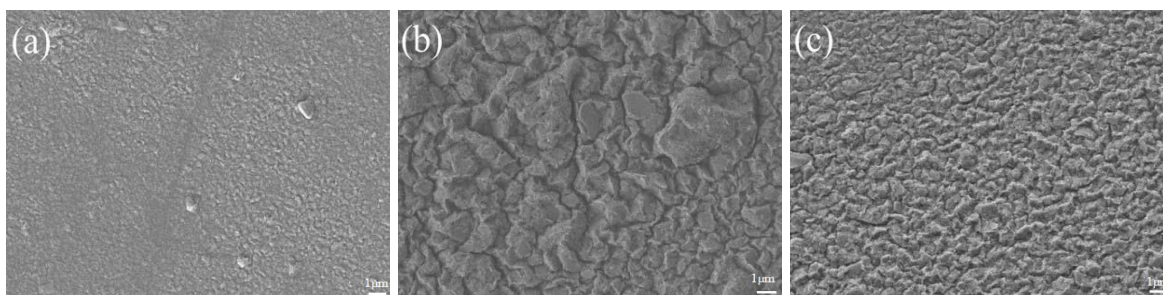
**Fig. 10.** Weight loss percentage *versus* duration from week 3 to week 9

The investigation on the surface morphologies of unfilled PVOH are illustrated in Fig. 11. Figure 11a and Fig. 11b show the PVOH thin film at the magnification power of 500 $\times$  and 5000 $\times$ , respectively. There were large smooth and fine surface areas that gave the transparency properties to the PVOH film (Chan *et al.* 2009).



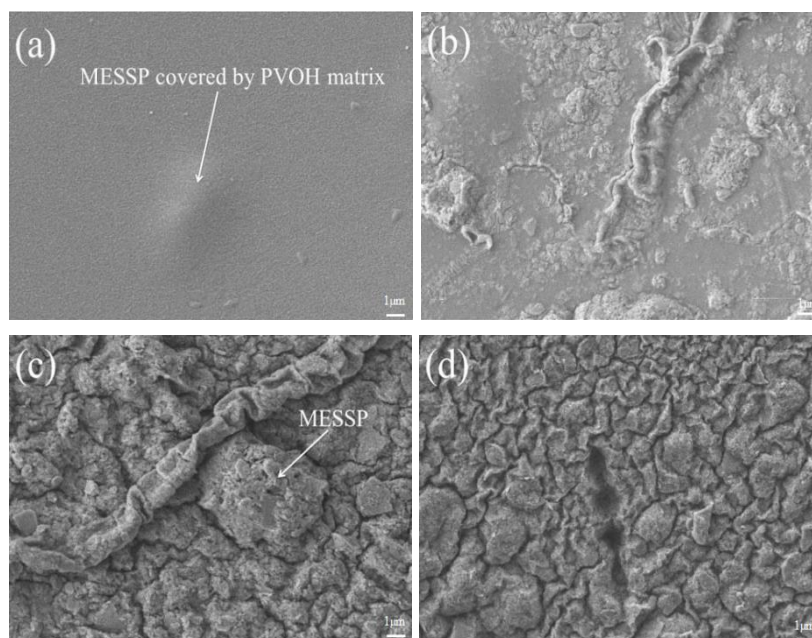
**Fig. 11.** SEM images of unfilled PVOH film before soil burial test at different magnification. (a) 500 $\times$  and (b) 5000 $\times$

Figure 12 displays the SEM micrographs scanned on the PVOH films after the soil burial test. The films started to wrinkle due to the swelling process. The generation of fold and wrinkles were increased on the PVOH films as the period of the PVOH films exposed to the moisture and water in the soil increased, which led to the higher degree of swelling and the water absorption (Kadajji and Betageri 2011). In addition, there was no growth of microorganisms or crack formation on the surface of the unfilled PVOH. Thus, Fig. 12 (a-c) confirmed that no biodegradation occurred.



**Fig. 12.** Comparison of surface morphology of unfilled PVOH after soil burial test at 5000 $\times$  magnification. (a) Week 3; (b) week 6; and (c) week 9

Figure 13 represents the SEM images of PVOH containing 10 wt % MESSP loading. Figure 13 (a) shows that the MESSP were fully covered by the matrix PVOH. The assumption of the good interaction and good adhesion between MESSP and PVOH matrix can be confirmed through this observation.



**Fig. 13.** Comparison of surface morphology of PVOH/MESSP 90/10 wt % at 5000 $\times$  magnification, before and after soil burial test. (a) Before soil burial test; (b) after week 3; (c) after week 6; and (d) after week 9

Based on Fig. 13b, it can be seen that the MESSP particles were partially visible on the surface of the matrix, which was damaged through the microbial activity. In week 9, the MESSP started to leach out from the matrix as shown in Fig. 13c, suggesting that fiber was utilized by microorganisms as a source of carbon and energy (Gu *et al.* 1996). The surface morphology of the composites was rougher at the end of week 9. The studies above stated that the rate of degradation was the highest for the 20 wt% loading of MESSP as this could be further demonstrated in the SEM images.

The observed patterns shown in Fig. 14 also provide evidence of degradation of the PVOH/MESSP films containing 20 wt% MESSP, as there were crack propagations formed on the surface of the composites. In addition, Fig. 15 also shows the ability of bacteria to attach and grow on the surface of the PVOH/MESSP films. The microorganisms will degrade the cellulose or lignocellulose found in the MESSP particles and eventually decompose the film. Thus, MESSP incorporated PVOH film were etched by the microorganisms where damages and the degradation happen (Ali *et al.* 2016).

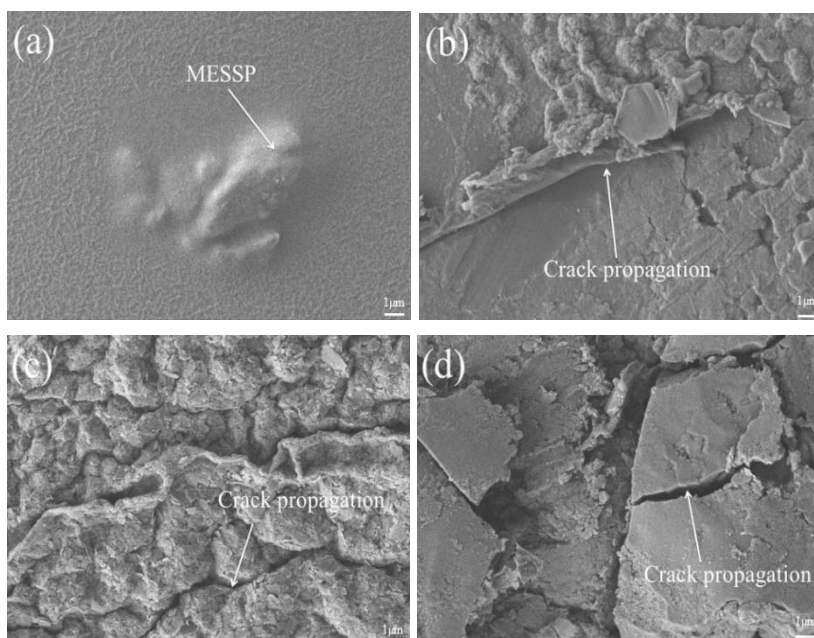


**Fig. 14.** Comparison of Surface Morphology of PVOH/MESSP 80/20 wt% at 5000× Magnification, before and after soil burial test. (a) Before soil burial test; (b) after week 3; (c) after week 6; and (d) week 9

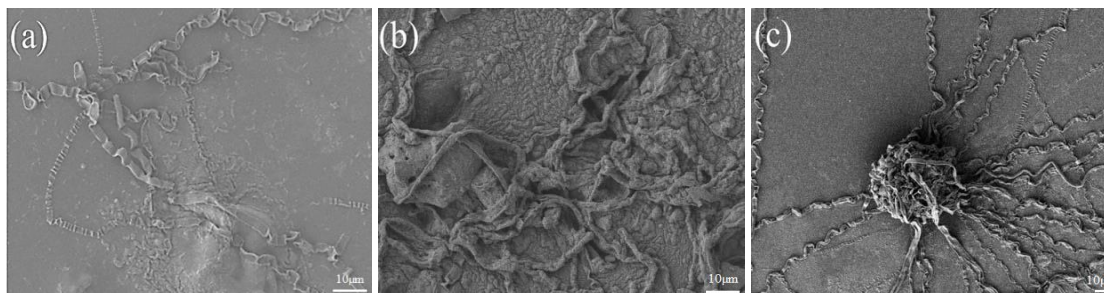


**Fig. 15.** Attachment of bacteria on the surface of the PVOH/MESSP 80/20 wt% Film after soil burial test. (a) after week 3; (b) after week 6; and (c) after week 9

The physical appearance of the samples was observed after the soil burial test to investigate their biodegradability. In Fig. 16, the degree of shrinkage was higher for the higher loading of the MESSP. Moreover, the degradation of the composite was more prominent in Fig. 16 (d) as the crack propagation illustrated in the SEM image caused the film to start to break into smaller pieces indicating biodegraded films.

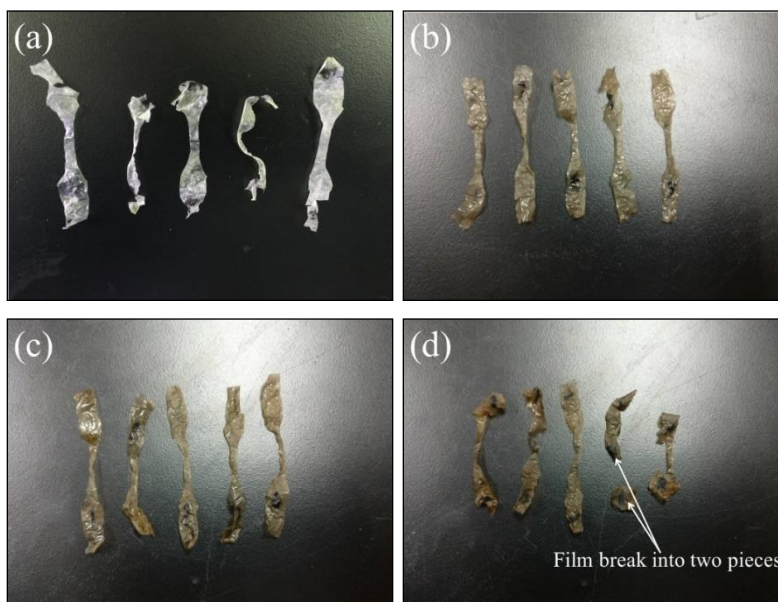


**Fig. 16.** Physical appearance of the composite films after week 9 of soil burial. (a) unfilled PVOH, (b) PVOH/MESSP 95/5 wt% (c) PVOH/MESSP 90/10 wt% (d) PVOH/MESSP 80/20 wt%

## CONCLUSIONS

1. The *Mimusops elengi* seed shell powder (MESSP) filled poly-(vinyl alcohol) (PVOH) films with an average thickness of 58.1  $\mu\text{m}$  were successfully produced through membrane casting at 0, 5, 10, 15, and 20 wt% of MESSP loading.
2. The MESSP and PVOH are compatible with each other because, as the ATR-FTIR analysis showed, both are hydrophilic in nature. The surface morphology of the PVOH was found to be smooth and fine where it gives the transparency properties. Moreover, MESSP particles have irregular shape and they were loosely arranged. The surface of the particles was flat and smooth and there was no pores and cracks that appeared.
3. The incorporation of the MESSP in the PVOH gave the negative effect on the tensile strength and elongation at break. The increasing loading of MESSP from 5 to 20 wt % blended films have lower tensile strength (46.2 to 26.8 MPa) and elongation at break (91.1 to 41.9%) than the unfilled PVOH (47.7 MPa and 129.2%). However, the tensile modulus was increased (970.3 MPa to 2192.4 MPa) with the increasing of the MESSP content from 5% to 20 wt% as compared to unfilled PVOH (270.6 MPa). In the surface fracture analysis, the aggregation of MESSP was observed at the higher loading of MESSP where voids were formed, which lead to poor filler/matrix interaction.
4. Water resistance was increased at higher MESSP loading as the water absorption

capacity was reduced from 842% to 488%.

5. The soil burial degradation test revealed that the addition of the MESSP in the PVOH matrix increased the degradation rate of the films as proved by the increasing of the weight loss of the films. The blended film deteriorated more at the higher loading of MESSP with a longer period of exposure time. As the evidenced observed from SEM images and physical appearance, cracks were formed on the surface at the same time that the films were starting to break into pieces.

## ACKNOWLEDGEMENTS

The authors thank University Tunku Abdul Rahman for providing all the necessary equipment to conduct this research.

## REFERENCES CITED

- Abdul Khalil, H., Poh, B., Jawaid, M., Ridzuan, R., Suriana, R., Said, M., Ahmad, F., and Nik Fuad, N. (2009). "The effect of soil burial degradation of oil palm trunk fiber-filled recycled polypropylene composites," *J. Reinf. Plast. Comp.* 29(11), 1653-1663. DOI: 10.1177/0731684409102939
- Alemdar, A., and Sain, M. (2008). "Isolation and characterization of nanofibers from agricultural residues – Wheat straw and soy hulls," *Bioresource Technol.* 99(6), 1664-1671. DOI: 10.1016/j.biortech.2007.04.029
- Ali, A., Shaker, K., Nawab, Y., Jabbar, M., Hussain, T., Militky, J., and Baheti, V. (2016). "Hydrophobic treatment of natural fibers and their composites—A review," *J. Ind. Text.* 47(8), 2153-2183. DOI: 10.1177/1528083716654468
- Asim, M., Abdan, K., Jawaid, M., Nasir, M., Dashtizadeh, Z., Ishak, M., and Hoque, M. (2015). "A review on pineapple leaves fibre and its composites," *Int. J. Polym. Sci.* 1-16. DOI: 10.1155/2015/950567
- ASTM D570-98 (2010). "Water absorption of plastics," ASTM International, West Conshohocken, PA.
- ASTM D638-14 (2014). "Tensile properties of plastics," ASTM International, West Conshohocken, PA.
- Bakar, N., Chee, C., Abdullah, L., Ratnam, C., and Ibrahim, N. (2015). "Thermal and dynamic mechanical properties of grafted kenaf filled poly (vinyl chloride)/ethylene vinyl acetate composites," *Material. Design* (1980-2015), 65, 204-211. DOI: 10.1016/j.matdes.2014.09.027
- Baliga, M., Pai, R., Bhat, H., Palatty, P., and Bloor, R. (2011). "Chemistry and medicinal properties of the Bakul (*Mimusops elengi* Linn): A review," *Food Res. Int.* 44(7), 1823-1829. DOI: 10.1016/j.foodres.2011.01.063
- Baschek, G., Hartwig, G., and Zahradnik, F. (1999). "Effect of water absorption in polymers at low and high temperatures," *Polymer* 40(12), 3433-3441. DOI: 10.1016/S0032-3861(98)00560-6
- Campos, A., Marconato, J., and Martins-Franchetti, S. (2011). "Biodegradation of blend films PVA/PVC, PVA/PCL in soil and soil with landfill leachate," *Braz. Arch. Biol. Techn.* 54(6), 1367-1378. DOI: 10.1590/S1516-89132011000600024

- Chan, K., Senin, H., Naimah, I., Rusop, M., and Soga, T. (2009). Structural and mechanical properties of polyvinyl alcohol (PVA) thin film,” *AIP Conf. Proc.* DOI: 10.1063/1.3160165
- Chauhan, A., and Chauhan, P. (2013). “Natural fibers and biopolymer,” *Journal of Chemical Engineering & Process Technology* s6. DOI: 10.4172/2157-7048.S6-001
- Das, G., and Biswas, S. (2016). “Physical, mechanical and water absorption behaviour of coir fiber reinforced epoxy composites filled with Al<sub>2</sub>O<sub>3</sub> particulates,” *IOP Conf. Ser.-Materials Sci.* 115 (1), 1-10. DOI: 10.1088/1757-899X/115/1/012012
- Espert, A., Vilaplana, F., and Karlsson, S. (2004). “Comparison of water absorption in natural cellulosic fibres from wood and one-year crops in polypropylene composites and its influence on their mechanical properties,” *Compos. Part A-Appl. S.* 35(11), 1267-1276. DOI: 10.1016/j.compositesa.2004.04.004
- Fan, M., Dai, D., and Huang, B. (2014). “Fourier transform infrared spectroscopy for natural fibres,” ([http://cdn.intechopen.com/pdfs/37067/InTech%5BHYPHEN%5DFourier\\_transform\\_infrared\\_spectroscopy\\_for\\_natural\\_fibres.pdf](http://cdn.intechopen.com/pdfs/37067/InTech%5BHYPHEN%5DFourier_transform_infrared_spectroscopy_for_natural_fibres.pdf)), Accessed 23 February 2018.
- Fern, K. (2017). “*Mimusops elengi* - Useful tropical plants,” (<http://tropical.theferns.info/viewtropical.php?id=Mimusops%20elengi>), Accessed 2 Aug. 2017.
- Gao, C., Ren, J., Wang, S., Sun, R., and Zhao, L. (2014). “Preparation of polyvinyl alcohol/xylan blending films with 1,2,3,4-butane tetracarboxylic acid as a new plasticizer,” *J. Nanomater.* 1-8. DOI: 10.1155/2014/764031
- Ghani, M., and Ahmad, S. (2011). “The comparison of water absorption analysis between counterrotating and corotating twin-screw extruders with different antioxidants content in wood plastic composites,” *Adv. Mater. Sci. Eng.* 1-4. DOI: 10.1155/2011/406284
- Gu, J., Ford, T., Thorp, K., and Mitchell, R. (1996). “Microbial growth on fiber reinforced composite materials,” *Int. Biodeter. Biodegr.* 37(3-4), 197-204. DOI: 10.1016/S0964-8305(96)00035-2
- Jeyasundari, J., Praba, P., Jacob, Y., Rajendran, S., and Kaleeswari, K. (2016). “Green synthesis and characterization of silver nanoparticles using *Mimusops elengi* flower extract and its synergistic antimicrobial potential,” *American Chemical Science Journal* 12(3), 1-11. DOI: 10.9734/ACSJ/2016/23161
- Kadajji, V., and Betageri, G. (2011). “Water soluble polymers for pharmaceutical applications,” *Polymers* 3(4), 1972-2009. DOI: 10.3390/polym3041972
- Kadam, P., Yadav, K., Deoda, R., Shivatare, R., and Patil, M. (2012). “*Mimusops elengi*: A review on ethnobotany, phytochemical and pharmacological profile,” *Journal of Pharmacognosy and Phytochemistry* 1(2278- 4136) (3), 64-71. DOI: vol1Issue3/Issue\_sept\_2012/10.1.pdf
- Kalambettu, A., Damodaran, A., Dharmalingam, S., and Vallam, M. (2014). “Evaluation of biodegradation of pineapple leaf fiber reinforced PVA composites,” *J. Nat. Fibers* 12(1), 39-51. DOI: 10.1080/15440478.2014.880104
- Krzeminski, J., and Molisak-tolwinska, H. (1991). “The structure of water-swollen poly(vinyl alcohol) and the swelling mechanism,” *J. Macromol. Sci. A.* 28(3-4), 413-429. DOI: 10.1080/00222339108052151
- Marsh, K., and Bugusu, B. (2007). “Food packaging—Roles, materials, and environmental issues,” *J. Food Sci.* 72(3), R39-R55. DOI: 10.1111/j.1750-3841.2007.00301.x

- Mendez-Sanchez, N., Cutright, T., and Qiao, P. (2004). "Accelerated weathering and biodegradation of E-glass polyester composites," *Int. Biodeter. Biodegr.* 54(4), 289-296. DOI: 10.1016/j.ibiod.2004.03.018
- Muniyadi, M., Ng, T., Munusamy, Y., and Ooi, Z. (2018). "Mimusops elengi seed shell powder as a new bio-filler for polypropylene-based bio composite," *BioResources* 13(1), 272-289. DOI: 10.15376/biores.13.1.272-289
- Nakasaki, K., Ohtaki, A., and Takano, H. (2000). "Biodegradable plastic reduces ammonia emission during composting," *Polym. Degrad. Stabil.* 70(2), 185-188. DOI: 10.1016/S0141-3910(00)00104-X
- Obasi, H., Igwe, I., and Madufor, I. (2013). "Effect of soil burial on tensile properties of polypropylene/plasticized cassava starch blends," *Adv. Mater. Sci. Eng.* 1-5. DOI: 10.1155/2013/326538
- Ooi, Z., Chan, K., Ewe, C., Muniyadi, M., Teoh, Y., and Ismail, H. (2017). "Evaluation of water affinity and soil burial degradation of thermoplastic film derived from oil palm ash-filled polyvinyl alcohol," *BioResources* 12(2). DOI: 10.15376/biores.12.2.4111-4122
- Ooi, Z., Ismail, H., Abdul Aziz, N., and Abu Bakar, A. (2011a). "Preparation and properties of biodegradable polymer film based on polyvinyl alcohol and tropical fruit waste flour," *Polym.-Plast. Technol.* 50(7), 705-711. DOI: 10.1080/03602559.2010.551391
- Ooi, Z., Ismail, H., Abu Bakar, A., and Aziz, N. (2011b). "Effects of jackfruit waste flour on the properties of poly(vinyl alcohol) film," *J. Vinyl. Addit. Techn.* 17(3), 198-208. DOI: 10.1002/vnl.20269
- Raj, B., K., U. S., and Siddaramaiah. (2004), "Low density polyethylene/starch blend films for food packaging applications," *Adv. Polym. Technol.* 23(1), 32-45. Doi:10.1002/adv.10068
- Ramaraj, B. (2006). "Crosslinked poly(vinyl alcohol) and starch composite films: Study of their physicomechanical, thermal, and swelling properties," *J. Appl. Polym. Sci.* 103(2), 1127-1132. DOI: 10.1002/app.24612
- Shi, J., Xing, D., and Lia, J. (2012). "FTIR studies of the changes in wood chemistry from wood forming tissue under inclined treatment," *Energ. Proced.* 16, 758-762. DOI: 10.1016/j.egypro.2012.01.122
- Singh, K., Srivastava, P., Kumar, S., Singh, D., and Singh, V. (2014). "Mimusops elengi Linn. (*Maulsari*): a potential medicinal plant," *Archives of Biomedical Sciences* 2 (1)(2300-7257), 18-29. DOI: papers/1600940047
- Siracusa, V., Dalla Rosa, M., and Iordanskii, A. (2017). "Performance of poly(lactic acid) surface modified films for food packaging application," *Materials* 10(8), 850. DOI: 10.3390/ma10080850
- Stuart, B. (2004). "Infrared Spectroscopy," Chichester, Eng.: J. Wiley
- Suki, F., Ismail, H., and Abdul Hamid, Z. (2013). "Preparation and properties of polyvinyl alcohol/banana frond flour biodegradable Film," *Rubber, Plastics and Recycling Technology* 30(2). DOI: 10.1177/147776061403000203
- Tan, B., Ching, Y., Poh, S., Abdullah, L., and Gan, S. (2015). "A Review of Natural Fiber Reinforced Poly(Vinyl Alcohol) Based Composites: Application and Opportunity," *Polymers* 7(11), 2205-2222. DOI: 10.3390/polym7111509
- Tardif, R. (2013). *The Life of a Plastic Bottle / Green Home Library*. [online] Greenhome.com. Available at: <http://www.greenhome.com/blog/the-life-of-a-plastic-bottle> [Accessed 29 Jun. 2017].

- Thakur, V., and Singha, A. (2010). "Mechanical and Water Absorption Properties of Natural Fibers/Polymer Biocomposites," *Polym.-Plast. Technol.* 49(7), 694-700. DOI: 10.1080/03602551003682067
- Thomas, S., Joseph, K., Malhotra, S., Goda, K., and Sreekala, M. (2012). *Polymer Composites, Volume 1, Macro- and Microcomposites*, Wiley VCH, Berlin. DOI: 10.1002/9783527645213
- Threepopnatkul, P., Kaerkitcha, N., and Athipongarporn, N. (2009). "Effect of surface treatment on performance of pineapple leaf fiber–polycarbonate composites," *Compos. Part B-Eng.* 40(7), 628-632. DOI: 10.1016/j.compositesb.2009.04.008
- Troedec, M., Sedan, D., Peyratout, C., Bonnet, J., Smith, A., Guinebretiere, R., Gloaguen, V., and Krausz, P. (2008). "Influence of various chemical treatments on the composition and structure of hemp fibres," *Compos. Part A-Applied S.* 39(3), 514-522. DOI: 10.1016/j.compositesa.2007.12.001
- Vanstrom, J. (2012). *Mechanical Characterization of Commercial Biodegradable Plastic Films*. Master's Thesis, Iowa State University, Ames, Iowa.
- Yee, T. W., Choy, L. J., and Rahman, W. A. W. A. (2011). "Mechanical and water absorption properties of poly(vinyl alcohol)/sago pith waste biocomposites," *J. Compos. Mater.* 45(11), 1201-1207.

Article submitted: May 1, 2018; Peer review completed: December 15, 2018; Revised version received and accepted: May 26, 2019; Published: May 31, 2019.

DOI: 10.15376/biores.14.3.5595-5614